Journal of Organometallic Chemistry, 272 (1984) 91–103
Elsevier Sequoia S.A., Lausanne – Printed in The Netherlands

SYNTHESIS OF THE CARBONYL CLUSTER DIANION $[RuRh_4(CO)_9(\mu_2\text{-}CO)_6]^{2-}$ AND X-RAY CRYSTAL STRUCTURE OF ITS BIS(TRIPHENYLPHOSPHINE)IMINIUM SALT

ALESSANDRO FUMAGALLI and GIANFRANCO CIANI

C.N.R., Centro di Studio sulla Sintesi e la Struttura dei Composti dei Metalli di Transizione nei Bassi Stati di Ossidazione, Via G. Venezian 21, 20133 Milano (Italy)

(Received March 22nd, 1984)

Summary

The dianion $[RuRh_4(CO)_{15}]^{2-}$ has been obtained by reductive carbonylation of mixtures of $Rh_4(CO)_{12}$ and $Ru_3(CO)_{12}$, and the bis(triphenylphosphine)iminium salt has been characterized by single-crystal X-ray diffraction techniques. Triclinic crystals, space group $P\bar{1}$ (No. 2), a 11.459(3), b 14.171(5), c 26.083(8) Å, α 84.32(3), β 83.46(2), γ 82.81(2)°, $Z = 2$; the salt is isomorphous with $(PPN)_2[RuIr_4(CO)_{15}]$. Least-squares refinement based on 2849 significant reflections gave a final R value of 0.059. The mixed metal cluster is an elongated trigonal bipyramid with the Ru atom located in apical position, as confirmed by variable temperature ^{13}C NMR spectroscopy. The mean values of the Rh_{eq}–Rh_{eq}, Rh_{eq}–Rh_{ap} and Rh_{eq}–Ru bond lengths are 2.71, 3.03 and 2.99 Å, respectively. The nine terminal and the six edge-bridging CO groups are disposed as in $[RuIr_4(CO)_{15}]^{2-}$.

Introduction

A renewed interest in homogeneous catalysis involving mixed metals systems, particularly Ru–Rh [1], and our specific interest in the peculiar reactivity of pentanuclear carbonyl clusters [2–6] led us to investigate the possible existence of a species such as $[RuRh_4(CO)_{15}]^{2-}$. This dianion has now been synthesized by a procedure very similar to that used in the case of $[RuIr_4(CO)_{15}]^{2-}$ [5] and structurally characterized in the solid state as well as in solution. It can be regarded as another member of a family of general formula $[MRh_4(CO)_{15}]^{n-}$ (M = Rh, $n = 1$; M = Fe, Ru, $n = 2$) [2,7], and its bis(triphenylphosphine)iminium (PPN^+) salt has been found to be isomorphous and isostructural with the corresponding salts of both $[RuIr_4(CO)_{15}]^{2-}$ [5] and $[FeRh_4(CO)_{15}]^{2-}$ [7b].

Results

The $[RuRh_4(CO)_{15}]^{2-}$ anion was produced by reduction in methanol, at room temperature and under 1 atm of CO, of mixtures of $Ru_3(CO)_{12}$ and $Rh_4(CO)_{12}$,

0022-328X/84/$03.00

involving progressive addition of NaOH up to approximately the 0.5 *M* concentration. The Ru/Rh metal ratios were varied in order to optimize the yields and, as previously observed for the mixed Ru–Ir system [5], it was found that acceptable yields were obtained only in the presence of an excess of Ru; use of a theoretical Ru/Rh ratio of 1/4 led to only very small amounts of the mixed metal cluster, the main products being Rh clusters, mainly $[Rh_6(CO)_{15}]^{2-}$ and $[Rh_7(CO)_{16}]^{3-}$ [8], and unidentified Ru species. It was only when the Ru/Rh ratio approached 1/1 that the mixed pentanuclear dianion could be isolated in high yields. The best preparation is carried out starting with equimolecular amounts of $Ru_3(CO)_{12}$ and $Rh_4(CO)_{12}$ (Ru/Rh = 1.00/1.33) and adding 1 *M* NaOH in methanol up to a ratio Ru/OH^- of approximately 1/7. At the end of the reaction, treatment with a slight excess of (PPN)Cl gives a precipitate of fairly pure $(PPN)_2[RuRh_4(CO)_{15}]$ in yields of up to 80% with respect to Rh.

The red mother liquor contains more soluble by-products, which can be precipitated by further addition of bulky cations and/or water. Following fractional crystallization of such a precipitate, $[Ru_3H(CO)_{11}]^-$, $[Rh(CO)_4]^-$, and possibly $[RuH(CO)_4]^-$, were recognized on the basis of the IR data reported in the literature [9–11].

The presence of both mononuclear and trinuclear Ru species at the end of the reaction, suggests that the excess of Ru may be required in order to obtain, in the complex equilibria present during the reduction, enough mononuclear Ru fragments to give condensation with some Rh species. In fact close IR monitoring of the reaction shows that at the early stages, the rhodium reacts on its own, yielding first $[Rh_6(CO)_{15}]^{2-}$ and then, as the reduction proceeds, $[Rh_7(CO)_{16}]^{3-}$; condensation

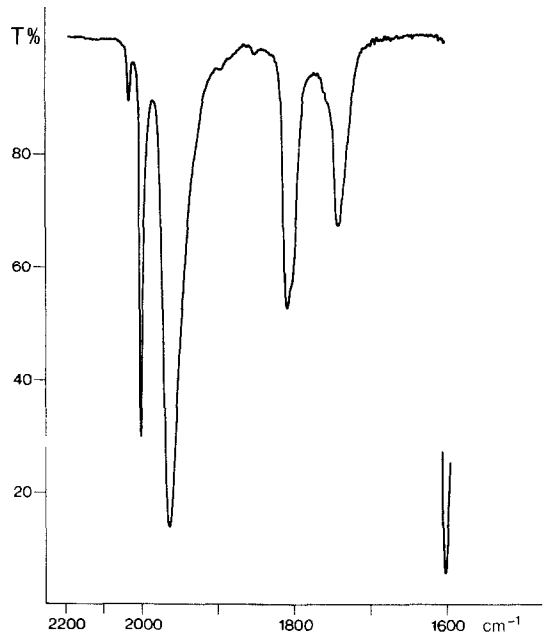

Fig. 1. IR spectrum of $(PPN)_2[RuRh_4(CO)_{15}]$ in THF under 1 atm CO; bands (cm^{-1}) at 2040w, 2005s, 1964ss, 1811ms, 1805sh, 1743m (w = weak, s = strong, m = medium, sh = shoulder).

with ruthenium then takes place at the end of the reduction, to yield ultimately the mixed metal dianion.

Crystals of $(PPN)_2[RuRh_4(CO)_{15}]$, suitable for X-ray diffraction, were obtained by the slow diffusion of 2-propanol into a THF solution under a CO atmosphere.

The almost exact agreement of the IR, recorded under CO atmosphere (Fig. 1), with that of $[FeRh_4(CO)_{15}]^{2-}$ [7] is noteworthy, as is the similarity of the band pattern with that of $[RuIr_4(CO)_{15}]^{2-}$ [5], though there is a significant high-frequency shift in the bridging CO stretching region.

The product, indefinitely stable in THF solution under CO, undergoes a little decomposition in vacuum or under nitrogen, a change in colour from clear orange-yellow to a darker brown-yellow being observed; re-exposure to CO quickly reverses the colour change. However, only a minor change can be detected in the IR spectrum recorded under nitrogen, with the appearance of just one additional weak band at 1992 cm^{-1}, and no change was detected in the ^{13}C NMR (see below). Crystallization under nitrogen by the slow diffusion technique again yielded crystals of $(PPN)_2[RuRh_4(CO)_{15}]$, with only trace amounts of a black unknown product.

Description of the structure

The structure of the anion is shown in Fig. 2. Bond distances and angles are listed in Tables 1 and 2, respectively. The structure contains a trigonal bipyramidal metal atom cluster, elongated in the direction of the ideal three-fold axis, as is usually

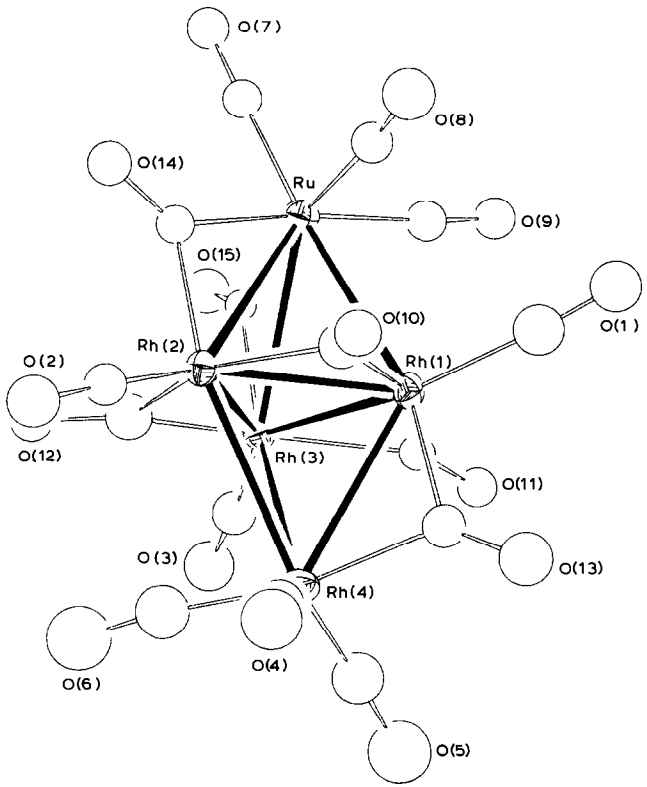

Fig. 2. Structure of the $[RuRh_4(CO)_{15}]^{2-}$ dianion. The carbonyls are indicated by their oxygen atoms.

TABLE 1

BOND DISTANCES (Å) IN $[RuRh_4(CO)_9(\mu\text{-}CO)_6](PPN)_2$ [a]

M–M		$M–C_{brd}$	
Ru–Rh(1)	2.962(3)	Ru–C(14)	2.10(2)
Ru–Rh(2)	2.998(2)	Ru–C(15)	2.09(2)
Ru–Rh(3)	3.005(2)	Rh(1)–C(10)	2.02(2)
Rh(1)–Rh(2)	2.721(3)	Rh(2)–C(10)	2.12(3)
Rh(1)–Rh(3)	2.728(2)	Rh(1)–C(11)	1.99(2)
Rh(2)–Rh(3)	2.683(2)	Rh(3)–C(11)	2.09(2)
Rh(1)–Rh(4)	2.926(2)	Rh(2)–C(12)	2.04(3)
Rh(2)–Rh(4)	3.061(3)	Rh(3)–C(12)	1.86(3)
Rh(3)–Rh(4)	3.099(2)	Rh(1)–C(13)	1.97(2)
		Rh(4)–C(13)	2.03(3)
$M–C_{ter}$		Rh(2)–C(14)	1.96(2)
Ru–C(7)	1.86(2)	Rh(3)–C(15)	1.99(2)
Ru–C(8)	1.90(2)		
Ru–C(9)	1.92(2)	$C_{ter}–O$	
Rh(1)–C(1)	1.85(3)	C(1)–O(1)	1.14(3)
Rh(2)–C(2)	1.78(2)	C(2)–O(2)	1.22(2)
Rh(3)–C(3)	1.78(3)	C(3)–O(3)	1.23(2)
Rh(4)–C(4)	1.84(3)	C(4)–O(4)	1.19(3)
Rh(4)–C(5)	1.74(3)	C(5)–O(5)	1.25(3)
Rh(4)–C(6)	1.78(3)	C(6)–O(6)	1.21(3)
		C(7)–O(7)	1.17(2)
		C(8)–O(8)	1.15(2)
		C(9)–O(9)	1.13(2)
$C_{brd}–O$			
C(10)–O(10)	1.19(2)		
C(11)–O(11)	1.20(2)		
C(12)–O(12)	1.29(3)		
C(13)–O(13)	1.20(3)		
C(14)–O(14)	1.19(2)		
C(15)–O(15)	1.23(2)		
Cations $(PPN)^+$			
P(1)–N(1)	1.56(2)		
P(2)–N(1)	1.57(2)		
P(3)–N(2)	1.56(2)		
P(4)–N(2)	1.61(2)		
P(1)–C [b]	1.81(1)		
P(2)–C [b]	1.81(1)		
P(3)–C [b]	1.83(1)		
P(4)–C [b]	1.81(1)		

[a] C_{brd} = bridging carbonyl; C_{ter} = terminal carbonyl. [b] Mean value.

found in this type of 76 valence electron clusters. The overall idealized symmetry of the anion is C_s, the mirror plane passing through the Ru, Rh(1) and Rh(4) atoms. There are nine terminally bonded CO groups, one for each of the three equatorial metals Rh(1), Rh(2) and Rh(3), and three on each of the apical metals Ru and Rh(4). Of the six edge-bridging carbonyls, three are located in almost coplanar positions on the central triangle edges, two others bridge the Ru atom to the two equatorial atoms Rh(2) and Rh(3), and the sixth connects the third equatorial Rh(1) atom to the apical Rh(4). The carbonyl stereochemistry is the same as that previously found in $[RuIr_4(CO)_{15}]^{2-}$ [5], in which the Ru atom was located unambigu-

TABLE 2

SELECTED BOND ANGLES (°) IN THE ANION $[RuRh_4(CO)_9(\mu\text{-}CO)_6]^{2-}$ [a]

M–M–M		Rh(4)–Rh(3)–C(15)	157.8(5)
Rh(1)–Ru–Rh(2)	54.33(6)	Ru–Rh(1)–C(13)	164.9(7)
Rh(1)–Ru–Rh(3)	54.42(6)	Rh(2)–Rh(4)–C(13)	90.4(7)
Rh(2)–Ru–Rh(3)	53.09(5)	Rh(3)–Rh(4)–C(13)	91.6(7)
Rh(1)–Rh(4)–Rh(2)	54.00(6)	Ru–Rh(1)–C(10)	86.0(7)
Rh(1)–Rh(4)–Rh(3)	53.76(5)	Ru–Rh(1)–C(11)	88.7(6)
Rh(2)–Rh(4)–Rh(3)	51.63(5)	Rh(4)–Rh(1)–C(10)	83.4(7)
Ru–Rh(1)–Rh(4)	121.30(8)	Rh(4)–Rh(1)–C(11)	81.1(6)
Ru–Rh(2)–Rh(4)	115.77(7)	Ru–Rh(2)–C(10)	83.3(6)
Ru–Rh(3)–Rh(4)	114.45(7)	Ru–Rh(2)–C(12)	84.7(7)
Rh(1)–Rh(2)–Rh(3)	60.65(6)	Rh(4)–Rh(2)–C(10)	78.4(6)
Rh(2)–Rh(1)–Rh(3)	58.98(6)	Rh(4)–Rh(2)–C(12)	83.6(7)
Rh(1)–Rh(3)–Rh(2)	60.37(6)	Ru–Rh(3)–C(11)	85.8(6)
		Ru–Rh(3)–C(12)	87.7(7)
		Rh(4)–Rh(3)–C(11)	75.5(5)
M–M–C_{brd}		Rh(4)–Rh(3)–C(12)	85.5(7)
Rh(1)–Ru–C(14)	91.9(6)		
Rh(1)–Ru–C(15)	93.0(5)		
Rh(4)–Rh(2)–C(14)	159.7(6)		
M–M–C_{ter}		Rh(4)–Rh(3)–C(3)	104.6(7)
Rh(1)–Ru–C(7)	174.1(6)	Rh(1)–Rh(4)–C(4)	108.3(8)
Rh(1)–Ru–C(8)	80.4(7)	Rh(1)–Rh(4)–C(5)	106.8(9)
Rh(1)–Ru–C(9)	78.5(7)	Rh(1)–Rh(4)–C(6)	126.9(8)
Rh(2)–Ru–C(7)	126.9(6)	Rh(2)–Rh(4)–C(4)	90.5(8)
Rh(2)–Ru–C(8)	93.3(6)	Rh(2)–Rh(4)–C(5)	146.3(9)
Rh(2)–Ru–C(9)	131.4(7)	Rh(2)–Rh(4)–C(6)	77.4(8)
Rh(3)–Ru–C(7)	131.4(7)	Rh(3)–Rh(4)–C(4)	142.1(8)
Rh(3)–Ru–C(8)	133.4(7)	Rh(3)–Rh(4)–C(5)	94.8(9)
Rh(3)–Ru–C(9)	91.8(6)	Rh(3)–Rh(4)–C(6)	80.9(8)
Ru–Rh(1)–C(1)	96.4(8)		
Rh(2)–Rh(1)–C(1)	144.2(8)		
Rh(3)–Rh(1)–C(1)	140.6(8)		
Rh(4)–Rh(1)–C(1)	142.3(8)		
Ru–Rh(2)–C(2)	143.9(7)		
Rh(1)–Rh(2)–C(2)	142.3(7)		
Rh(3)–Rh(2)–C(2)	144.0(7)		
Rh(4)–Rh(2)–C(2)	100.0(7)		
Ru–Rh(3)–C(3)	140.3(7)		
Rh(1)–Rh(3)–C(3)	141.8(8)		
Rh(2)–Rh(3)–C(3)	148.2(8)		
C–M–C		C(3)–Rh(3)–C(15)	97.6(9)
C(7)–Ru–C(8)	93.8(9)	C(11)–Rh(3)–C(15)	103.5(8)
C(7)–Ru–C(9)	101.3(9)	C(12)–Rh(3)–C(15)	88.1(9)
C(8)–Ru–C(9)	89.5(9)	C(4)–Rh(4)–C(5)	123.1(12)
C(14)–Ru–C(7)	87.9(9)	C(4)–Rh(4)–C(6)	90.3(11)
C(15)–Ru–C(7)	92.8(8)	C(5)–Rh(4)–C(6)	102.6(13)
C(14)–Ru–C(8)	85.6(9)	C(4)–Rh(4)–C(13)	89.8(10)
C(15)–Ru–C(8)	172.7(9)	C(5)–Rh(4)–C(13)	87.5(11)
C(14)–Ru–C(9)	169.9(9)	C(6)–Rh(4)–C(13)	167.8(11)
C(15)–Ru–C(9)	86.1(8)		
C(14)–Ru–C(15)	97.9(7)		
C(1)–Rh(1)–C(10)	101.9(11)		
C(1)–Rh(1)–C(11)	100.0(10)		
C(1)–Rh(1)–C(13)	98.6(11)		

(continued)

TABLE 2 (continued)

C(10)–Rh(1)–C(13)	89.0(9)		
C(11)–Rh(1)–C(13)	90.6(9)	M–C_{brd}–M	
C(2)–Rh(2)–C(10)	100.0(9)	Rh(1)–C(10)–Rh(2)	82.3(9)
C(2)–Rh(2)–C(12)	104.8(10)	Rh(1)–C(11)–Rh(3)	84.1(8)
C(2)–Rh(2)–C(14)	100.3(9)	Rh(2)–C(12)–Rh(3)	86.7(11)
C(10)–Rh(2)–C(14)	99.0(9)	Rh(1)–C(13)–Rh(4)	94.1(11)
C(12)–Rh(2)–C(14)	90.2(9)	Ru–C(14)–Rh(2)	95.3(10)
C(3)–Rh(3)–C(11)	97.7(10)	Ru–C(15)–Rh(3)	94.9(8)
C(3)–Rh(3)–C(12)	102.7(11)		
M–C–O (brd)		M–C–O (ter)	
Rh(1)–C(10)–O(10)	143(2)	Rh(1)–C(1)–O(1)	175(3)
Rh(2)–C(10)–O(10)	132(2)	Rh(2)–C(2)–O(2)	175(2)
Rh(1)–C(11)–O(11)	141(2)	Rh(3)–C(3)–O(3)	174(2)
Rh(3)–C(11)–O(11)	135(2)	Rh(4)–C(4)–O(4)	177(3)
Rh(2)–C(12)–O(12)	127(2)	Rh(4)–C(5)–O(5)	170(3)
Rh(3)–C(12)–O(12)	146(2)	Rh(4)–C(6)–O(6)	166(2)
Rh(1)–C(13)–O(13)	131(2)	Ru–C(7)–O(7)	177(2)
Rh(4)–C(13)–O(13)	135(2)	Ru–C(8)–O(8)	175(2)
Rh(2)–C(14)–O(14)	131(2)	Ru–C(9)–O(9)	174(2)
Ru–C(14)–O(14)	134(2)		
Rh(3)–C(15)–O(15)	129(1)		
Ru–C(15)–O(15)	136(2)		

[a] C_{brd} = bridging carbonyl; C_{ter} = terminal carbonyl.

ously. This justifies our assumption about the location of Ru, which is almost impossible to establish directly in the present case on the basis of X-ray data, because of the very similar scattering power of Ru and Rh. The assumption has been also confirmed by ^{13}C NMR analysis (see below). An analogous geometry is present also in the $[FeRh_4(CO)_{15}]^{2-}$ anion, because of isomorphism of the $(PPN)^+$ salts [7b].

The metal–metal bonds, ranging in the interval 2.683(2)–3.099(2) Å, have the following mean values: (i) within the equatorial Rh(1,2,3) triangle, 2.71 Å; (ii) Rh–Rh bonds involving the apical Rh(4) 3.03 Å; (iii) Ru–Rh, 2.99 Å. This pattern is similar to that observed in $[RuIr_4(CO)_{15}]^{2-}$, the main difference being that the Ir–Ru bond lengths were slightly longer (mean 3.01 Å) than the Ir_{eq}–Ir_{ap} ones (mean 3.00 Å).

A curious feature, noted previously for the corresponding interactions in $[RuIr_4(CO)_{15}]^{2-}$, is that the two Ru–Rh carbonyl bridged edges are longer than the unbridged one (3.00 vs. 2.96 Å), while the Rh(1)–Rh(4) bridged edge is, as expected, shorter than the two Rh(2,3)–Rh(4) unbridged edges (2.93 vs. 3.08 Å).

A comparison of mean bond lengths within the four related 76 electron trigonal bipyramidal species, $[RuRh_4(CO)_{15}]^{2-}$, $[RuIr_4(CO)_{15}]^{2-}$ [5], $[Rh_5(CO)_{14}I]^{2-}$ [6] (with an iodine replacing a terminal CO of one apical metal) and $[Rh_5(CO)_{15}]^{-}$ [2] (where one apical-equatorial bridging CO becomes a terminal group bonded to an equatorial metal) is given in Table 3. The metal–metal bond lengths are very similar in the four species. Almost all the metal–carbonyl interactions within the monoanion are longer than in the three dianions, as expected for reduced back-donation. In these three species a common feature is the asymmetry of the two bridging carbonyls

TABLE 3

COMPARISONS BETWEEN MEAN BOND LENGTHS (Å) IN RELATED TRIGONAL BIPYRAMIDAL CLUSTERS [a]

	$[RuRh_4(CO_{15}]^{2-}$	$[RuIr_4(CO)_{15}]^{2-}$	$[Rh_5(CO)_{14}I]^{2-}$	$[Rh_5(CO)_{15}]^{-}$ [b]
$M_{eq}-M_{eq}$	2.71	2.71	2.71	2.73
$M_{eq}-M_{ap2}$	2.99	3.01	2.98	2.97
$M_{eq}-M_{ap1}$	3.03	3.00	2.97	
$M_{eq}-C_{ter}$	1.80	1.72	1.83	1.91
$M_{ap2}-C_{ter}$	1.89	1.86	1.88	1.97
$M_{ap1}-C_{ter}$	1.79	1.70	1.89	
$M_{eq}-C_{ee}$	2.02	2.00	2.09	2.16
$M_{eq}-C_{ae}$	1.97	1.97	1.95	2.00
$M_{ap2}-C_{ae}$	2.10	2.12	2.09	2.11
$M_{ap1}-C_{ae}$	2.03	1.86	2.14	
$C_{ter}-O$	1.19	1.26	1.18	1.10
$C_{brd}-O$	1.22	1.32	1.18	1.10

[a] M_{eq} = equatorial metal; M_{ap1} = apical metal connected to one bridging CO group; M_{ap2} = apical metal connected to two bridging CO groups; C_{ter} = terminal carbonyl; C_{brd} = bridging carbonyl; C_{ee} = bridging carbonyl in equatorial position; C_{ae} = apical-equatorial bridging carbonyl. [b] In this anion the two apical metals are equivalent.

bonded to the same apical metal, with $M_{eq}-C_{ae}$ bonds shorter than the $M_{ap2}-C_{ae}$ ones.

^{13}C NMR spectra

The 20 MHz ^{13}C NMR spectrum at $-103°C$ in THF-d_8 of a sample of $(PPN)_2[RuRh_4(CO)_{15}]$ (about 30% ^{13}CO enriched and recorded in CO atmosphere) is shown in Fig. 3. This spectrum provides the most convincing proof (not directly obtainable by the X-ray analysis) of the apical location of the ruthenium atom.

The terminal CO's region (180–220 ppm) shows several resonances which can all

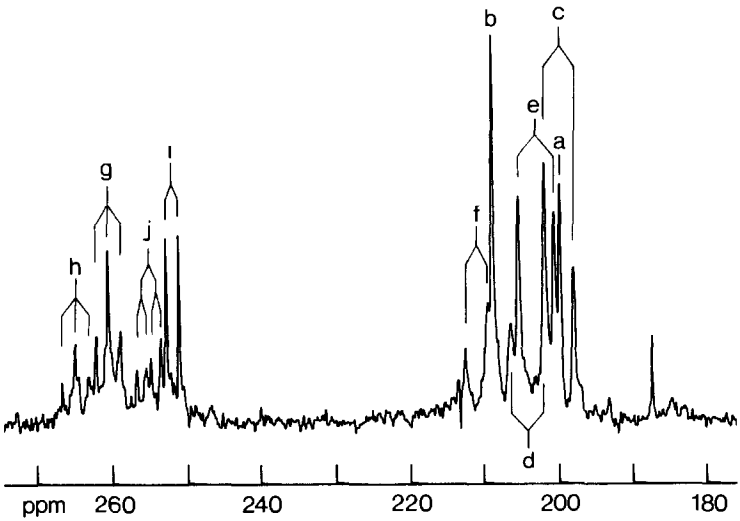

Fig. 3. ^{13}C NMR spectrum of $(PPN)_2[RuRh_4(CO)_{15}]$ in THF-d_8 under CO (30% ^{13}CO) at $-103°C$.

TABLE 4

COMPARISON OF ^{13}C NMR CHEMICAL SHIFTS FOR $[RuRh_4(CO)_{15}]^{2-}$ AT −103 °C AND $[FeRh_4(CO)_{15}]^{2-}$ AT −86 °C (J(Rh–C) in Hz) [a]

	$RuRh_4(CO)_{15}]^{2-}$	$[FeRh_4(CO)_{15}]^{2-}$
C_a	199.7 s	216.3 s
C_b	208.6 s	217.3 s
C_c^*	199.8 (77.6) d	} 200.5 (91.5) d
C_e^*	202.8 (95.0) d	
C_d^{**}	ca. 204 (ca. 92) d	} 201.3 (91.6) d
C_f^{**}	210.8 (60.2) d	
C_g	260.5 (32.5) t	259.4 (30.5) t
C_h	264.9 (ca. 35) t	263.5 (36.6) t
C_i	252.0 (34.6) d	253.5 (33.6) d
C_j	255.2 (25.6, ca. 39) d + d	250.4 (25.9, 39.7) d + d

[a] s = singlet, d = doublet, t = triplet. Assignments * and ** may be interchanged.

be assigned in terms of the diagramatic structure depicted in Fig. 4. Two singlets at 199.7 and 208.6 ppm (intensity ratio 1/2) are due to the three carbonyls bonded to the apical Ru, C_a and C_b, respectively; they lie quite far apart, compared with what is found for the analogous iron-bonded carbonyls in $[FeRh_4(CO)_{15}]^{2-}$ (see Table 4). Also the resonances due to the carbonyls terminally bonded to the rhodium atoms appear separately, in contrast with observations on the Fe–Rh species, and C_c and C_e give rise to two well distinct doublets at 199.8 ppm (J 77.6 Hz) and at 202.8 ppm (J 95.0 Hz); their absolute assignment is, of course, impossible without selective Rh decoupling, and therefore C_c and C_e may be interchanged. The two small doublets at

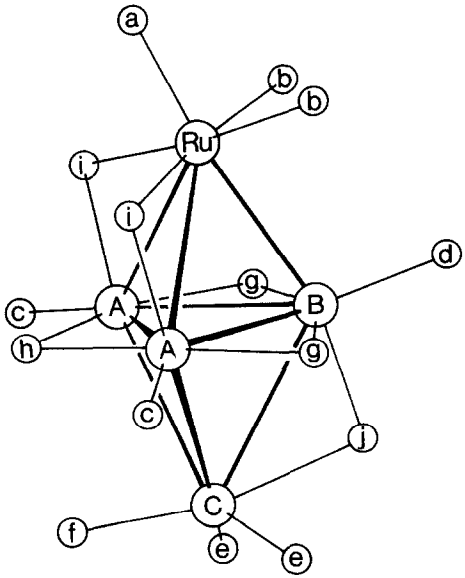

Fig. 4. Schematic representation of the structure of $[RuRh_4(CO)_{15}]^{2-}$.

ca. 204 ppm (J ca. 92 Hz) and 210.8 ppm (J 60.2 Hz) are due to C_d and C_f and here too we are not able to label them, unambiguously.

The bridging CO region (250–270 ppm) is also entirely consistent with the structure in Fig. 4; the well resolved doublet of intensity 2 at 252.0 ppm ($^1J(Rh_A–C_i)$ 34.6 Hz) can be unambiguously assigned to C_i, bridging Rh_A and the apical ruthenium, while the other signal of intensity 2 at 260.5 ppm ($^1J(Rh_{A\text{-}B}–C_g)$ 32.5 Hz) is due to the two equivalent C_gO ligands bridging in the equatorial plane Rh_A and Rh_B, with very similar J values making it roughly a triplet. The two resonances of intensity 1 have been assigned respectively to C_h bridging in the equatorial plane (triplet at 264.9 ppm, $^1J(Rh_A\text{-}C_h)$ 35.4 Hz), and C_j bridging between the apical Rh_C and the equatorial Rh_B (doublet of doublets at 255.2 ppm, $^1J(Rh_{B,C}–C_j)$ 25.6 and ca. 39 Hz). As can be seen from Table 4, the chemical shifts found for C_g, C_h and C_i agree well with those obtained for $[FeRh_4(CO)_{15}]^{2-}$ [7] (resepectively 259.4 (30.5), 263.5 (36.6) and 253.5 (33.6)) but this is not the case for the signal from C_j (250.4 (39.7 and 25.9)), which shows in our compound a significant shift to low frequencies. The assignments were confirmed by a high resolution 50 MHz spectrum at $-90\,°C$.

Fluxional behaviour was noted upon raising the temperature, both the terminal and the bridging region showing progressive collapse into very broad resonances. At room temperature the collapse in the terminal region is almost complete, while in the bridging region a triplet (^1J(Rh–C) 33.2 Hz) becomes visible at 260.6 ppm; the signal eventually emerges at $+55\,°C$ as a sharper peak against a broad large signal (maximum at about 214 ppm), the integration ratio being about 1/4. This could be due, as previously suggested in the Fe–Rh case [7], to both the equatorial C_g and C_h and the Rh_A and Rh_B atoms becoming equivalent by migration of the other twelve carbonyls.

The variable-temperature spectra were also recorded under a nitrogen atmosphere, and at $-103\,°C$ only the low intensity singlet at 187.2 ppm, assigned to the free CO in solution, had become undetectable, the general features of the spectra being the same as under CO.

Experimental

All the operations were carried out under N_2 or CO (as specified) in carefully purified solvents. $Rh_4(CO)_{12}$ was prepared by the literature method [12], while $Ru_3(CO)_{12}$ was obtained commercially. Infrared spectra were recorded on a Perkin–Elmer 781 spectrophotometer using 0.1 mm CaF_2 cells previously purged with CO or N_2. The ^{13}CO enriched sample was obtained by direct exchange at room temperature with 90% ^{13}CO, using standard vacuum-line technique and variable temperature ^{13}C NMR spectra were recorded on a Bruker WP80 multinuclear spectrophotometer.

Synthesis of $[PPN]_2[RuRh_4(CO)_{15}]$

$Ru_3(CO)_{12}$ (0.157 g, 0.245 mmol) and $Rh_4(CO)_{12}$ (0.183 g, 0.245 mmol) were placed in a Schlenk tube and the system was evacuated and filled with CO. Methanol (10 ml) was then added and after 10 min of stirring, required to saturate the solution with CO, the mixture was treated with NaOH (1 M in MeOH, 5 ml) and stirred vigorously with a magnetic bar a slight positive CO pressure being maintained by means of a mercury valve. After 20 h the brown-yellow solution obtained

was treated dropwise with a solution of (PPN)Cl (1 g in 8 ml MeOH) to give a precipitate of yellow flakes. The precipitate was filtered off from the red mother liquor under CO, washed with 2-propanol (3 × 10 ml), and briefly vacuum dried. Extraction with THF (10 ml) under CO gave a product with a fairly good IR spectrum; slow diffusion of 2-propanol (40 ml) into this solution, carried out under CO, gave orange crystals of the product. Yield 0.384 g (78% based on Rh).

X-Ray analysis

Crystal data. $C_{87}H_{60}N_2O_{15}P_4Rh_4Ru$, $M = 2010.0$, Triclinic, a 11.459(3), b 14.171(5), c 26.083(8) Å, α 84.32(3), β 83.46(2), γ 82.81(2)°, U 4159.5 Å^3, D_c 1.605 g cm^{-3} for $Z = 2$, $F(000) = 2000$, Mo-K_α radiation (λ 0.71073 Å), μ(Mo-K_α) 10.78 cm^{-1}. Space group $P\bar{1}$ (No. 2).

Intensity data collection and refinements. A flat single crystal of dimensions 0.05 × 0.19 × 0.26 mm was mounted on an Enraf-Nonius CAD4 automated diffractometer and the setting angles of 25 random intense reflections, in the range $16° < 2\theta < 22°$, were used to determine by least-squares fit the accurate cell parameters and orientation matrix. The data collection was performed, using graphite-monochromated Mo-K_α radiation, by the ω-scan method, in a hemisphere within the limits $3 < \theta < 20.5°$. A variable scan-speed (from 2.5 to 20° min^{-1}) and a variable scan-range of $(0.8 + 0.35 \tan\theta)°$ were used, with a 25% extension at each end of the scan-range for background determination. The total number of collected reflections was 7843. The intensities of three standard reflections were measured every 2 h, and showed a significant decay of the sample, of ca. 20% by the end of the collection. The intensities were corrected for Lorentz, polarization and decay effects. An empirical absorption correction was applied, based on ψ-scans (ψ 0–360° every 10°) of suitable reflections with χ values close to 90°; the maximum, minimum and average relative transmission values were 1.00, 0.89 and 0.93, respectively. A set of 2849 independent significant reflections, with $I > 2\sigma(I)$, was used in the refinements of the structure.

The initial coordinates of the metal atoms were assumed to be the same as those previously obtained for the isomorphous salt $(PPN)_2[RuIr_4(CO)_{15}]$ [5]. The location of the Ru atom was also assumed to be the same, i.e. in one of the two capping positions of the trigonal bipyramid. Difference-Fourier maps showed all the remaining non-hydrogen atoms in positions very close to those of the corresponding atoms in the $[RuIr_4(CO)_{15}]^{2-}$ species. The refinements were carried out by full-matrix least-squares methods. Anisotropic thermal factors were assigned only to the metal atoms and to the P atoms. The hydrogen atoms of the phenyl groups were ignored. Weights were assigned according to the formula $w = 1/\sigma^2(F_0)$, with $\sigma(F_0) = \sigma(F_0^2)/2F_0$ and $\sigma(F_0^2) = [\sigma^2(I) + (AI)^2]^{1/2}/\mathrm{Lp}$, the fudge factor A being assumed equal to 0.03.

The final values of the conventional R and R_w agreement indices were 0.059 and 0.064, respectively. The final difference-Fourier map did not show significant residual peaks. All computations were performed on a PDP 11/34 computer, using the Enraf-Nonius Structure Determination Package (SDP) and the physical constants therein tabulated.

The final positional parameters are given in Table 5. The final list of observed and calculated structure factors moduli and anisotropic and isotropic thermal parameters can be obtained by application to the authors.

(Continued on p. 103)

TABLE 5

FINAL POSITIONAL PARAMETERS FOR $(PPN)_2[RuRh_4(CO)_{15}]$

Atom	x	y	z
Rh(1)	0.5703(2)	0.3285(1)	−0.30378(8)
Rh(2)	0.5456(2)	0.2119(1)	−0.21479(8)
Rh(3)	0.3932(2)	0.3702(1)	−0.22745(8)
Rh(4)	0.3775(2)	0.2092(2)	−0.29769(9)
Ru	0.6407(2)	0.3981(2)	−0.20975(9)
P(1)	0.1505(6)	−0.1878(4)	−0.1309(3)
P(2)	0.2565(6)	−0.1705(5)	−0.0347(3)
P(3)	0.0892(6)	0.2050(5)	0.3541(3)
P(4)	0.2095(5)	0.1802(4)	0.4483(3)
O(1)	0.750(2)	0.421(1)	−0.3771(8)
O(2)	0.558(2)	0.007(1)	−0.1728(8)
O(3)	0.142(2)	0.460(1)	−0.2073(8)
O(4)	0.484(2)	0.009(2)	−0.3214(9)
O(5)	0.188(2)	0.306(2)	−0.361(1)
O(6)	0.222(2)	0.149(2)	−0.205(1)
O(7)	0.736(1)	0.468(1)	−0.1188(7)
O(8)	0.886(2)	0.324(1)	−0.2578(8)
O(9)	0.638(1)	0.582(1)	−0.2811(7)
O(10)	0.734(1)	0.141(1)	−0.2990(7)
O(11)	0.389(1)	0.495(1)	−0.3298(7)
O(12)	0.351(1)	0.244(1)	−0.1287(7)
O(13)	0.519(2)	0.259(1)	−0.3987(8)
O(14)	0.694(1)	0.224(1)	−0.1345(7)
O(15)	0.418(2)	0.506(1)	−0.1533(7)
N(1)	0.228(2)	−0.153(1)	−0.0927(7)
N(2)	0.191(1)	0.171(1)	0.3891(7)
C(1)	0.678(3)	0.387(2)	−0.350(1)
C(2)	0.558(2)	0.090(2)	−0.191(1)
C(3)	0.246(2)	0.427(2)	−0.218(1)
C(4)	0.442(3)	0.087(2)	−0.311(1)
C(5)	0.268(3)	0.274(2)	−0.332(1)
C(6)	0.295(3)	0.164(2)	−0.240(1)
C(7)	0.701(2)	0.438(2)	−0.154(1)
C(8)	0.792(2)	0.354(2)	−0.242(1)
C(9)	0.638(2)	0.512(2)	−0.257(1)
C(10)	0.665(2)	0.204(2)	−0.283(1)
C(11)	0.435(2)	0.431(2)	−0.303(1)
C(12)	0.398(2)	0.274(2)	−0.174(1)
C(13)	0.498(2)	0.262(2)	−0.353(1)
C(14)	0.646(2)	0.261(2)	−0.170(1)
C(15)	0.467(2)	0.449(1)	−0.1838(9)
C(111)	0.048(2)	−0.090(1)	−0.1515(9)
C(112)	0.048(2)	−0.000(2)	−0.134(1)
C(113)	−0.036(2)	0.076(2)	−0.152(1)
C(114)	−0.108(2)	0.062(2)	−0.191(1)
C(115)	−0.113(2)	−0.028(2)	−0.207(1)
C(116)	−0.031(2)	−0.105(2)	−0.188(1)
C(121)	0.241(2)	−0.225(2)	−0.189(1)
C(122)	0.340(2)	−0.169(2)	−0.204(1)
C(123)	0.403(3)	−0.202(2)	−0.255(1)
C(124)	0.371(2)	−0.273(2)	−0.279(1)
C(125)	0.278(2)	−0.324(2)	−0.260(1)
C(126)	0.208(2)	−0.301(2)	−0.213(1)

(continued)

TABLE 5 (continued)

Atom	x	y	z
C(131)	0.073(2)	−0.290(2)	−0.1016(9)
C(132)	0.135(2)	−0.377(2)	−0.100(1)
C(133)	0.067(2)	−0.456(2)	−0.075(1)
C(134)	−0.047(2)	−0.432(2)	−0.060(1)
C(135)	−0.111(2)	−0.343(2)	−0.060(1)
C(136)	−0.053(2)	−0.267(2)	−0.087(1)
C(211)	0.381(2)	−0.260(1)	−0.0277(9)
C(212)	0.429(2)	−0.311(2)	−0.070(1)
C(213)	0.521(2)	−0.382(2)	−0.064(1)
C(214)	0.572(2)	−0.399(2)	−0.017(1)
C(215)	0.531(2)	−0.349(2)	0.0256(9)
C(216)	0.432(2)	−0.278(1)	0.0198(9)
C(221)	0.129(2)	−0.205(1)	0.0088(9)
C(222)	0.142(2)	−0.293(2)	0.043(1)
C(223)	0.036(2)	−0.311(2)	0.077(1)
C(224)	−0.066(2)	−0.247(2)	0.074(1)
C(225)	−0.071(2)	−0.170(2)	0.040(1)
C(226)	0.026(2)	−0.141(2)	0.0059(9)
C(231)	0.293(2)	−0.062(1)	−0.0134(9)
C(232)	0.262(2)	−0.042(2)	0.040(1)
C(233)	0.303(2)	0.038(2)	0.056(1)
C(234)	0.359(2)	0.102(2)	0.019(1)
C(235)	0.391(2)	0.082(2)	−0.031(1)
C(236)	0.353(2)	−0.003(2)	−0.050(1)
C(311)	−0.015(2)	0.301(2)	0.377(1)
C(312)	−0.127(2)	0.286(2)	0.399(1)
C(313)	−0.207(3)	0.364(2)	0.414(1)
C(314)	−0.165(3)	0.457(2)	0.412(1)
C(315)	−0.048(3)	0.472(2)	0.392(1)
C(316)	0.030(2)	0.391(2)	0.372(1)
C(321)	0.155(2)	0.246(1)	0.2889(9)
C(322)	0.092(2)	0.319(2)	0.258(1)
C(323)	0.141(2)	0.344(2)	0.206(1)
C(324)	0.240(2)	0.298(2)	0.187(1)
C(325)	0.302(2)	0.223(2)	0.218(1)
C(326)	0.258(2)	0.195(2)	0.271(1)
C(331)	0.013(2)	0.100(2)	0.346(1)
C(332)	−0.085(2)	0.119(2)	0.317(1)
C(333)	−0.142(3)	0.040(2)	0.308(1)
C(334)	−0.101(2)	−0.054(2)	0.328(1)
C(335)	−0.002(2)	−0.063(2)	0.354(1)
C(336)	0.055(2)	0.012(2)	0.3662(9)
C(411)	0.277(2)	0.069(2)	0.4768(9)
C(412)	0.354(2)	0.010(1)	0.4424(9)
C(413)	0.411(2)	−0.077(2)	0.465(1)
C(414)	0.399(2)	−0.100(2)	0.518(1)
C(415)	0.324(2)	−0.042(2)	0.553(1)
C(416)	0.262(2)	0.043(2)	0.530(1)
C(421)	0.071(2)	0.212(2)	0.4888(9)
C(422)	−0.003(2)	0.137(2)	0.494(1)
C(423)	−0.119(2)	0.160(2)	0.524(1)
C(424)	−0.149(2)	0.246(2)	0.543(1)
C(425)	−0.070(3)	0.320(2)	0.537(1)

TABLE 5 (continued)

Atom	x	y	z
C(426)	0.040(2)	0.297(2)	0.507(1)
C(431)	0.303(2)	0.271(2)	0.4526(9)
C(432)	0.340(2)	0.288(2)	0.499(1)
C(433)	0.417(2)	0.360(2)	0.501(1)
C(434)	0.458(2)	0.400(2)	0.455(1)
C(435)	0.427(2)	0.388(2)	0.406(1)
C(436)	0.348(2)	0.316(2)	0.405(1)

Acknowledgements

We thank Dr. S. Martinengo of C.N.R. Milano for helpful discussions and Mrs. M. Bonfà of Universitá di Milano for recording NMR spectra.

References

1 R. Whyman, Phil. Trans. R. Soc. Lond. A 308 (1982) 131.
2 A. Fumagalli, T.F. Koetzle, F. Takusagawa, P. Chini, S. Martinengo and B.T. Heaton, J. Amer. Chem. Soc., 102 (1980) 1740.
3 A. Fumagalli, S. Martinengo, P. Chini, D. Galli, B.T. Heaton and R. DellaPergola, Inorg. Chem., (1984) in press.
4 A. Fumagalli, G. Longoni, P. Chini, A. Albinati and S. Bruckner, J. Organomet. Chem., 202 (1980) 329.
5 A. Fumagalli, T.F. Koetzle and F. Takusagawa, J. Organomet. Chem., 213 (1981) 365.
6 S. Martinengo, G. Ciani and A. Sironi, J. Chem. Soc. Chem. Commun., (1979) 1059.
7 (a) A. Ceriotti, G. Longoni, R. DellaPergola, B.T. Heaton and D.O. Smith, J. Chem. Soc., Dalton Trans., (1983) 1433; (b) A. Ceriotti, G. Longoni, M. Manassero, M. Sansoni, R. DellaPergola, B.T. Heaton and D.O. Smith, J. Chem. Soc., Chem. Commun., (1982) 886.
8 S. Martinengo and P. Chini, Gazz. Chim. Ital., 102 (1972) 344.
9 B.F.G. Johnson, J. Lewis, P.R. Raithby and G. Suss, J. Chem. Soc., Dalton Trans., (1979) 1356.
10 P. Chini and S. Martinengo, Inorg. Chim. Acta, 3 (1969) 21.
11 H.W. Walker and P.C. Ford, J. Organomet. Chem., 214 (1981) C43.
12 S. Martinengo, G. Giordano and P. Chini, Inorg. Synth., 20 (1980) 209.